J. Fluid Mech. (1993), *vol.* 254, *pp.* 417–435

Global density effects on the self-preservation behaviour of turbulent free jets

By C. D. RICHARDS† AND W. M. PITTS

National Institute of Standards and Technology, Building and Fire Research Laboratory, Gaithersburg, MD 20899, USA

(Received 13 May 1992 and in revised form 15 March 1993)

An experimental investigation was designed to test the hypothesis that all axisymmetric turbulent free jets become asymptotically independent of the source conditions and may be described by classical similarity analysis. Effects of initial conditions were studied by varying jet exit boundary conditions and the global density ratio. The exit velocity profile and turbulence level was changed by using both pipe and nozzle flow hardware. Initial density differences were imposed by using three gases: helium, methane, and propane. The scalar field (concentration) in the momentum-dominated regime of the far field (10 to 60 jet exit diameters downstream) of turbulent free jets was characterized using Rayleigh light scattering as the diagnostic. The results show that regardless of the initial conditions axisymmetric turbulent free jets decay at the same rate, spread at the same angle, and both the mean and r.m.s. values collapse in a form consistent with full self-preservation. The means and fluctuations follow a law of full self-preservation in which two virtual origins must be specified. The two displacements are required to account for the effects of a finite source of momentum and different development of the velocity and mass distributions in the near fields of the jets. The memory of the jet is embodied in these two virtual origins.

1. Introduction

Similarity concepts are widely used in fluid engineering to describe various aspects of turbulent flow fields. Any number of textbooks can be consulted for discussions (e.g. see White 1974; Hinze 1975). Despite the advanced development and widespread use of these concepts, there is a great deal of confusion and controversy in the literature concerning their application. In this paper the findings from an experimental investigation of mixing in variable-density axisymmetric jets are used to characterize the similarity behaviour of these flow fields in regions well beyond the potential core where the turbulent flow is fully developed.

The turbulent variable-density jet has broad engineering importance and has been the subject of numerous investigations (see Abramovich 1963; Harsha 1971; Chen & Rodi 1980; and Gouldin *et al.* 1986 for reviews). Despite the large number of investigations reported in the literature, many uncertainties remain concerning both qualitative and quantitative properties of these flows.

The fact that constant-density turbulent jets exhibit self-preserving behaviour in the far field has been generally accepted. Recently, Dowling & Dimotakis (1988, 1990) have confirmed this behaviour in a careful investigation of constant-density axisymmetric jets. It was shown that the mean, root-mean-square (r.m.s.), and

† Current address: Department of Mechanical and Materials Engineering, Washington State University, Pullman, WA 99164-2920, USA.

probability density functions of a passive scalar obey similarity relations. In addition, concentration fluctuation power spectra were also collapsed by the use of self-similar variables. Dowling (1991) has analysed the same data and has shown that an estimate for the scalar dissipation rate is also collapsed in terms of appropriate similarity parameters.

It has not been verified, however, whether axisymmetric jets having global density variations (i.e. the jet and ambient fluids have different densities) achieve a full self-preserving state in the far field. Measurements for the rate of fall-off of the centreline concentration with downstream distance have yielded a range of values (see Pitts 1991*a*). There is also conflicting evidence in the literature concerning the attainment of an asymptotic value of the centreline unmixedness (the ratio of the r.m.s. to mean value of scalar). Pitts (1991*a*) found that an asymptotic value was reached regardless of the initial density ratio. Schefer & Dibble (1986), in contrast, did not observe an asymptote in the centreline unmixedness for a flow of propane into air. Based on a review of the literature and Schefer & Dibble's findings, Gouldin *et al.* (1986) concluded in their review of mixing in axisymmetric jets that variable-density jets do not attain asymptotic states. These conflicting results call into question whether variable-density jets can achieve a self-preserving asymptotic state.

Physically, self-similarity (or self-preservation) implies that the flow has reached a dynamic equilibrium or asymptotic state in which the mean and higher-order moments evolve together (Townsend 1976). In the classical view the asymptotic condition depends only on the rate of momentum addition and is independent of other initial conditions (Townsend 1976). Thus the source of the asymptotic jet can be viewed as a point source of momentum which has a mass flux of zero. Mathematically, a flow is self-similar when profiles of concentration (and velocity) can be collapsed by the choice of suitable scales for concentration (velocity) and length. Consequently, for an axisymmetric jet, the number of independent variables is reduced by one, and the governing equations are transformed to a set of ordinary differential equations.

Self-similarity is not possible for flows in which the density varies appreciably across the flow; that is, self-preserving solutions do not exist for the governing equations. In an axisymmetric jet with an initial density different than that of the ambient, density gradients decrease rapidly with downstream distance owing to the entrainment process, and the flow approaches a state in which the density ratio between the local jet fluid and the ambient ($R_{\rho l} = \rho_l/\rho_\infty$, where ρ_l and ρ_∞ are the local jet and ambient densities, respectively) approaches unity. In this region the assumption that density variations are important only in the buoyancy term (the Boussinesq approximation) can be applied to the governing equations and self-preserving solutions may be obtained. Great care is taken in this investigation to ensure that measurements are made in the momentum-dominated regime, and thus the buoyancy term is negligible. For this case the governing equations become identical to those for a constant-density axisymmetric turbulent jet.

The concentration (mole fraction), X, is measured in binary gas jets using Rayleigh light scattering. The density, ρ, is related to the mole fraction by

$$\rho = \rho_\infty(1-X)+\rho_0 X, \tag{1}$$

where ρ_0 is the density at the jet exit and ρ_∞ is the density of the surroundings. The mixture fraction or mass fraction, Y, can then be expressed as

$$Y = \frac{\rho_0 X}{\rho_\infty(1-X)+\rho_0 X} = \frac{R_\rho X}{1+(R_\rho-1)X}, \tag{2}$$

where R_ρ is the density ratio ρ_0/ρ_∞. Mass fraction is the appropriate concentration scalar for characterizing mixing in variable-density flows (Pitts & Kashiwagi 1984).

Similarity solutions for the velocity and scalar fields in an axisymmetric turbulent jet are obtained for Reynolds equations which are simplified by (i) neglecting molecular effects (i.e. high Reynolds number), (ii) invoking the boundary-layer approximations, and (iii) neglecting terms involving the fluctuations of density ($\overline{\rho' u'v'}, \overline{\rho' v'}, \overline{\rho' Y'}$, etc). These assumptions are valid in the far-field region of the jet.

From the simplified Reynolds equations similarity solutions are obtained by selecting scales for length, velocity and mass fraction; applying dimensional analysis and conservation of momentum and the scalar (mass fraction); and invoking the constant-entrainment hypothesis (Morton, Taylor & Turner 1956; Chen & Rodi 1980).

This analysis requires that self-similar solutions for the mass fraction satisfy

$$\frac{\mathrm{d}\delta_Y(z)}{\mathrm{d}z} = A, \qquad \bar{Y}(z,0)\frac{\delta_Y(z)}{r_\epsilon} = B, \tag{3}$$

where $\delta_Y(z)$ is the characteristic lengthscale (in this study taken to be the half-width at half-maximum of the radial mass fraction profile), $\bar{Y}(z,0)$ is the mean centreline mass fraction, r_ϵ is the effective radius, and A and B are constants. Chen & Rodi (1980) provide a summary of one approach for deriving these expressions.

Equation (3) requires that the jet growth be linear in z and the centreline decay of mass fraction be inversely proportional to z. The self-preserving profile of mean mass fraction is

$$\bar{Y}(z,\eta) = \frac{Y_0 r_\epsilon}{K_c(z-z_0)} f(\eta), \tag{4}$$

where K_c is the rate of centreline decay and is found from experiment (note that K_c has been included in the denominator to maintain conformity with earlier work from our laboratory (Pitts 1991*a*, *b*)), Y_0 is the initial mass fraction, z_0 is the virtual origin and is found from experiment, η is the non-dimensional radial coordinate $r/(z-z_0)$, and f is a smooth function. Note that K_c will be a universal constant for jets which have achieved a self-similar state. Y_0 is the mass fraction of the species of interest in the undiluted jet fluid. For jets of a single fluid, as in the experiments reports here, $Y_0 = 1$.

The effective-radius concept has been used by many researchers (Thring & Newby 1953; Becker, Hottel & Williams 1967; Avery & Faeth 1975; Dahm & Dimotakis 1987; Dowling & Dimotakis 1990; and Pitts 1991*a*). In this paper the effective radius is defined to be

$$r_\epsilon = \frac{m_0}{(\pi\rho_\infty J_0)^{\frac{1}{2}}}, \tag{5}$$

where m_0 is the initial mass flux and J_0 is the momentum flux for the jet. Physically, r_ϵ is the radius of a hypothetical jet with density ρ_∞ and the same m_0 and J_0 as the jet under consideration. If the velocity profile is uniform at the jet exit, then r_ϵ takes the form given by Thring & Newby (1953), $r_0(\rho_0/\rho_\infty)^{\frac{1}{2}}$ (r_0 is the nozzle or pipe radius, and ρ_0 is the initial density of the jet fluid). The form for r_ϵ is derived from dimensional arguments.

The centreline decay of the scalar required for similarity (that the inverse centreline value is linear in z) has been used in the literature to fit centreline data from axisymmetric jets with an initial density difference due to heating of jet fluid (i.e. Sunavala, Hulse & Thring 1957; Wilson & Danckwerts 1964; Sforza & Mons 1978) and gas composition (i.e. Birch *et al.* 1978; Gouldin *et al.* 1986; So *et al.* 1990; and Pitts

1991*a*). Measured values of K_c generally agree within an average deviation of $\pm 10\%$ (see Pitts 1991*a*). It has not been clarified whether these deviations are the result of experimental uncertainties or a breakdown in the similarity assumptions.

Past studies of variable-density jets have suggested that there may be a breakdown in similarity. If similarity holds, values of K_c should be independent of the initial density ratio of jet and ambient gases, $R_\rho = \rho_0/\rho_\infty$. Schefer & Dibble (1986) and Pitts (1991*a*) conclude that values of K_c are weakly dependent on R_ρ. They attribute this observation to a density effect not accounted for by the use of r_ϵ as the non-dimensionalizing lengthscale. The data of Niwa *et al.* (1984) show a similar correlation between K_c and density ratio.

The virtual origin, z_0, which appears in (4) allows near-field effects to be incorporated into the far-field description of the flow field. It is included to account for the experimental observation that the spatial location of the point source of momentum, which gives rise to the similarity solution of (4), often does not correspond to the nozzle exit ($z = 0$). The location of z_0 is known to be sensitive to initial conditions at the jet exit (Thring & Newby 1953; Chen & Rodi 1980; Pitts 1991*a*, *b*).

The goal of this study is to test the hypothesis that axisymmetric jets become asymptotically independent of source conditions. Effects of initial conditions are investigated by varying the jet exit boundary conditions and the global density ratio, R_ρ. Initial density differences are imposed by using three different jet gases: helium, methane, and propane. The exit velocity profile and turbulence level are varied by using both pipe and contoured nozzle flow hardware.

2. Experimental system

The scalar fields of axisymmetric jets with varying global density ratios and initial velocity profiles were characterized using Rayleigh light scattering (RLS) as the diagnostic. By careful experimental design it was possible to acquire measurements in the far fields of free turbulent jets where the local density ratio of the jet fluid to ambient ($R_{\rho l}$) approached unity and the flows were momentum dominated (i.e. buoyancy effects were negligible).

2.1. *Flow facility*

The experiments were performed in the quiescent environment of a cylindrical clean room. The facility, dubbed the Rayleigh Light Scattering Facility (RLSF), was carefully designed to minimize interferences associated with glare and Mie scattering. This facility is described in detail in Bryner, Richards & Pitts (1992). A schematic is shown in figure 1. The clean room system is composed of a 2.4 m tall $\times$ 2.4 m diameter cylindrical test section, high-efficiency particulate (HEPA) filters, and air distribution duct work and associated fans and exhaust. During operation the RLSF is completely isolated from the surrounding laboratory environment. Two variable-speed fans are used to flow air through the filters and test section and thus provide a clean environment in the test section. In the experiments described here, measurements were made in a quiescent environment by turning the filter blowers off and waiting for flow transients to dissipate. The filters do not remove gaseous contaminates such as the helium, propane, and methane used in the experiments. As a result the test section must be purged and filled with clean air after each experiment. The flow duct work is connected to the laboratory exhaust system for this purpose.

Two exit boundary conditions were used in the experiments: jets produced by a turbulent pipe flow, and jets produced by a contoured nozzle. In the majority of the

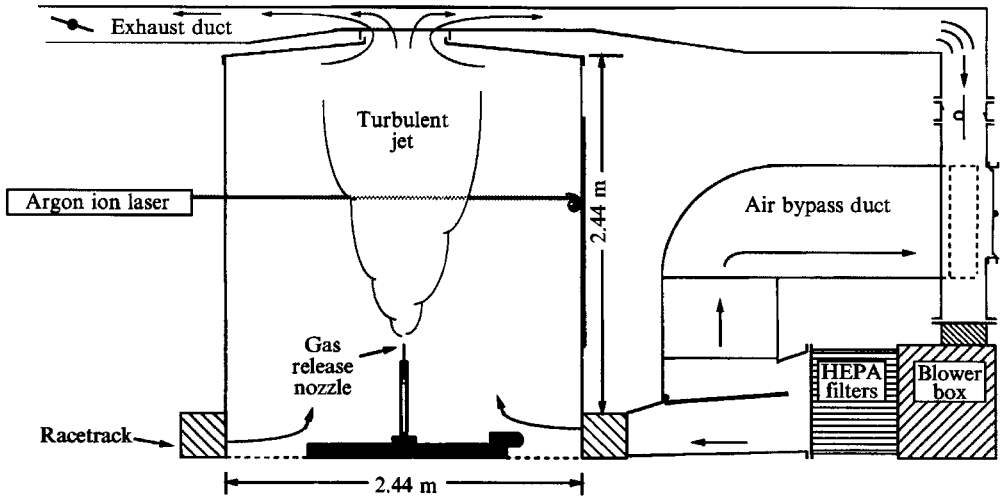

FIGURE 1. A schematic of the Rayleigh Light Scattering Facility.

experiments the turbulent pipe flow exit condition was used. The flow hardware consists of a 6.35 mm I.D. pipe with a sharp-edged exit. The same pipe as used in earlier experiments in this laboratory (Pitts & Kashiwagi 1984; Pitts 1991*a*, *b*) for jet measurements in the presence of a coflow was employed with the coflow glass enclosure removed. The length of the pipe is sufficient to ensure fully developed turbulent pipe flow at the exit. The flow assembly is mounted on a three-axis, computer-controlled positioning traverse placed on the floor of the test section. The pipe is mounted along the z-axis and the gas issues upward into the enclosure as shown in figure 1. Jet gas is supplied from pressurized tanks and is filtered to remove oil, moisture, and particulates. A mass flow controller is used to meter the gas.

Measurements were also recorded for a propane jet produced by a contoured nozzle with an I.D. of 6.35 mm and an area contraction ratio of 100:1. The nozzle was designed to have a 'top-hat' velocity profile at the exit with low turbulence intensity. The inner nozzle contour is a fitted fifth-order polynomial. The nozzle is preceded by a flow straightening and conditioning section consisting of a section of honeycomb and screens to dampen velocity fluctuations. The nozzle was designed, fabricated, and constructed in-house.

2.2. *Diagnostic*

RLS was used to measure real-time concentration (mole fraction) in the turbulent jets. The optical system is very similar to that described previously (Pitts & Kashiwagi 1984). An argon ion laser operating on all lines at a nominal power of 20 W is used to induce RLS. The beam enters the RLSF through a Brewster-angle window (to minimize reflections) and is then focused by a 250 mm focal length lens to a narrow waist with a diameter of 50 μm. The receiving optics are positioned perpendicular to the laser beam. The scattered light is collected by an f/2 lens system and imaged 1:1 onto a 400 μm pinhole which defines the length of the observation volume. After passing through the pinhole the scattered light is imaged onto the photocathode of a Thorn EMI Model 9781B photomultiplier tube (PMT).†

† Certain commercial equipment, instruments or materials are identified in this paper in order to adequately specify the experimental procedure. Such identification does not imply recommendation or endorsement by the National Institute of Standards and Technology, nor does it imply that the materials or equipment are necessarily the best available for the purpose.

The current output of the PMT is converted to a voltage across a 24 kΩ resistor, which is then fed to an Ithaco Model 4302 dual filter used as a low-pass 10 × amplifier. A cut-off frequency of 10 kHz was used, thus defining the Nyquist frequency. The signal is then passed to a 12 bit digitizer interfaced to a Masscomp 5450 computer. At each location 32000 points are acquired at a sampling rate of 20 kHz. The data are then stored on the hard disk for post processing.

During an experiment, the laser power was monitored and sampled simultaneously with the Rayleigh signal by recording the intensity of scattered laser light from the Brewster-angle window with a photodiode. This allowed minor laser power drift and fluctuations (1–2%) to be normalized out of the measurements.

Concentration measurements were performed in the manner described previously (Bryner, Richards & Pitts 1992). The RLS intensity is first calibrated by recording the average scattering signal from the ambient gas (air) and the jet gas (I_1 and I_2, respectively). The turbulent flow is then initiated and the real-time RLS signal, $I(t)$, recorded. The time behaviour of the mole fraction for the reservoir gas, $X_2(t)$, in the observation region is then determined from

$$X_2(t) = \frac{I(t) - I_1}{I_2 - I_1}. \tag{6}$$

Data reduction consists of converting mole fractions to mass fractions and then ensemble averaging to obtain mean and r.m.s. values.

2.3. *Experimental design*

The gases selected for the study were helium, methane, and propane. The Reynolds number (Re) for the flow is defined as

$$Re = D_0 U_0 / \nu_0, \tag{7}$$

where ν_0 is the kinematic viscosity of the jet gas, D_0 is the diameter of the jet exit, and U_0 is the average velocity at the jet exit ($U_0 = Q/(\pi D_0^2/4)$, where Q is the volume flow rate). Re for the helium jet was 4000, and for the other gases 25000. Higher Re for the helium flows were difficult to achieve due to the high exit velocities required. To estimate the axial position at which buoyancy forces begin to be important, the non-dimensional buoyancy lengthscale defined by Chen & Rodi (1980) was used

$$z_b = F^{-\frac{1}{2}} \left(\frac{\rho_0}{\rho_\infty}\right)^{-\frac{1}{4}} \left(\frac{z}{D_0}\right), \tag{8}$$

where F is the Froude number ($F = \rho_0 U_0^2 / g D_0 |\rho_\infty - \rho_0|$ and g is the gravitational constant). Chen & Rodi (1980) suggest that the flow is momentum dominated for values of $z_b < 0.53$, whereas the results of Papanicolaou & List (1988) show that jets are momentum dominated for $z_b < 1$. In this study, a conservative approach has been adopted and $z_b = 0.5$ was selected for the cut-off of the momentum-dominated region of the jet.

Measurements were acquired across the diameter of each jet at a minimum of three axial locations. Typically the axial stations corresponded to $z/r_0 = 40$, 60, and 80, although measurements were acquired further upstream for helium and further downstream for propane. At these downstream distances the local density ratio of the

Gas	R_ρ	Re	(z/r_0) @ $z_b = 0.5$	r_e, mm	Exit BC
Helium	0.138	4000	80	1.159	pipe
Methane	0.554	25000	150	2.334	pipe
Propane	1.552	25000	130	3.871	pipe
Propane	1.552	25000	130	3.918	nozzle

TABLE 1. Experimental parameters (BC denotes boundary condition)

jet to ambient fluid is approaching unity. Typically, at $z/r_0 = 40$ the local time-averaged density ratio on the centreline (i.e. $\bar{\rho}(z, 0)/\rho_\infty$) was approximately $1.00 \pm 10\%$ for all gases.

In the evaluation of the effective radius, r_e, for the pipe flow the momentum flux was computed using a power law formulation for the velocity profile (Schlichting 1979). The nozzle was designed to produce a thin boundary layer and consequently a top-hat profile was assumed for the exit velocity profile.

The operating conditions and relevant experimental parameters for each of the gases are presented in table 1.

3. Results and discussions

3.1. *Mean mass fraction*

Radial profiles of the mean mass fraction, $\bar{Y}(z, r)$, for the turbulent free jet of helium ($Re = 4000$) are shown in figure 2 for $z/r_0 = 20$, 40, 60, and 80. Similar results were obtained for the other gases. Gaussian curves were fit to each of the profiles and interpolation performed to obtain the mass fraction half-width, $r_{\frac{1}{2}}$. Half-widths of mass fraction at each axial location were determined for each of the gases and are shown in figure 3. In agreement with the requirements for self-preserving solutions, all the jets spread linearly. The graph shows that for a given downstream distance, the lighter gases have spread more. The angle of spread in the measurement region, however, appears to be identical for all of the gases except the propane jet produced from pipe flow. The angle of this jet is less than for the others. If, however, the first point at $z/r_0 = 40$ is discarded, the slope begins to fall in line with the other cases. This result is interpreted as evidence that the propane pipe flow jet requires a longer flow distance for the spreading angle to become constant.

Results from linear least-squares fits for the spreading rates are presented in table 2. The lines are characterized by $z_{0,J}$, the virtual origin (hypothetical axial location where the mass fraction half-width is zero), and m, the spreading rate as a function of z (i.e. tangent of the spreading half-angle, θ_c). Values of m are, within experimental uncertainty, identical for the four jets. Two sets of numbers appear for the propane jet issuing from a pipe to reflect the observation that this jet had not reached full development at $z/r_0 = 40$. The numbers in parentheses correspond to the fit of data at all axial positions. The other numbers are for fits excluding data at $z/r_0 = 40$.

There have been numerous measurements of the spreading rates of passive scalars for axisymmetric jets reported in the literature. Table 3 compares the results for many of these. The results cover a range of $m = 0.096$ to 0.13 which is roughly $\pm 15\%$ of the values included in table 2. There is no apparent correlation with Re, R_ρ, or the boundary conditions at the jet exit. The scatter is reduced considerably if only measurements recorded after 1982 are considered. Note that agreement between the

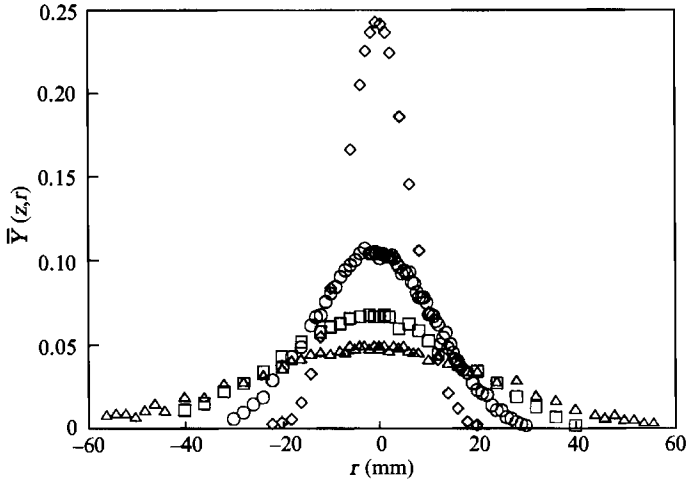

FIGURE 2. Radial profiles of the mean helium mass fraction for $z/r_0 = 20$ (◇), 40 (○), 60 (□), and 80 (△).

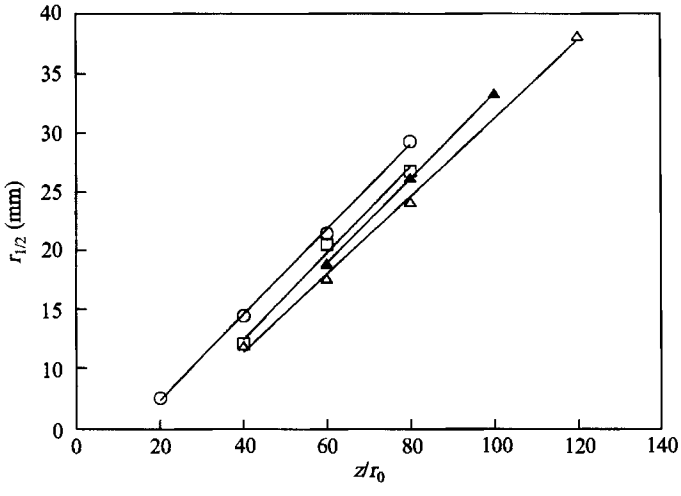

FIGURE 3. Concentration half-widths, $r_{\frac{1}{2}}$, for helium (○), methane (□), propane pipe (△), and propane nozzle (▲).

Gas	Exit BC	Slope, m	z_{0J}/r_0
Helium	pipe	0.113 ± 0.002	-0.30 ± 0.19
Methane	pipe	0.115 ± 0.009	5.7 ± 2.8
Propane	pipe	0.108 ± 0.002 (0.104)	8.5 ± 0.8 (5.0)
Propane	nozzle	0.113 ± 0.009	7.2 ± 0.4

TABLE 2. Virtual origins and spreading rates

current measurements of spreading rate in variable-density jets and the recent constant-density results of Dowling & Dimotakis (1990) is excellent. Based on reviews of the literature, Fischer *et al.* (1979) recommend a value of 0.106 for m while Chen & Rodi (1980) suggest a value of 0.11.

Reference	Passive scalar	Re	R_ρ	Exit BC	m	Range (r_0)
Hinze & van der Hegge Zijnen (1947)	temperature gases	67000	0.91, 1.09	pipe	0.97	16–40
		67000	≈ 1.0		0.96	16–40
Sunavala *et al.* (1957)	temperature, gases	17900–56900	0.48–1.0	short pipe	0.113	not reported
Wilson & Danckwerts (1964)	temperature	20000–40000	0.60–0.93	nozzle	0.13	40–110
Becker *et al.* (1967)	small particles	54000	1.0	nozzle	0.106	40–80
Birch *et al.* (1978)	natural gas	16000	0.56	pipe	0.097	40–80
Grandmaison *et al.* (1982)	small particles	270000	1.0	pipe	0.105	40–80
Namazian *et al.* (1988)	methane	7000	0.55	pipe	0.11	not reported
So *et al.* (1990)	helium/air mixture	4300	0.64	nozzle	0.107	18–49
Dowling & Dimotakis (1990)	ethylene into nitrogen	5000	1.002	nozzle	0.114	40–160
	propane into argon	16000	1.053	nozzle	0.114	60–180

TABLE 3. Spreading rate measurements reported in the literature

Gas	K_c	z_{0Y}/r_0
Helium	0.106±0.002	6.0±0.5
Methane	0.106±0.008	7.2±2.5
Propane (pipe)	0.104±0.007	−4.2±2.2
Propane (nozzle)	0.105±0.009	3.1±7.8

TABLE 4. Fitted values for the centreline decay law

The quantity z_{0J} is interpreted here as the virtual origin of momentum; that is, z_{0J} is the point source of momentum for self-similar behaviour. Experimentally it is observed that the ratio between the spreading rates of velocity and scalar, $\delta_U(z)/\delta_Y(z)$, is constant. Given that both $\delta_U(z)$ and $\delta_Y(z)$ are linear functions of z, it follows that the virtual origins must coincide. The data of So *et al.* (1990) show the virtual origins based on the spreading behaviour of velocity and mass fraction coincide.

A comparison of values of z_{0J} in table 2 reveals two interesting effects. First, the virtual origins for methane and propane (both nozzle and pipe) flows are relatively close to each other compared to the helium jet, which has a negative virtual origin located near the nozzle. In the absence of any density effect this may be explained by the difference in *Re*, i.e. *Re* for the helium jet is 4000 whereas for the other jets it is 25000. It has been shown that virtual origins for both inverse average velocity and inverse mass fraction along the jet centreline shift downstream with increasing *Re* (Harsha 1971; Pitts 1991*b*).

The second effect results from a comparison of the virtual origins of the propane jets for the two boundary conditions. The virtual origin for the pipe flow is downstream of that for the nozzle flow, which is consistent with the conclusion that the propane pipe jet has not attained an asymptotic spreading rate at $z/r_0 = 40$ while the flow from the nozzle appears to be fully developed. This result is somewhat counterintuitive. The nozzle flow might be expected to take longer to develop than the pipe flow due to the initial condition of low turbulence energy.

To test if the data obey full similarity relations (4), the centreline scaling law for each jet,

$$\frac{Y_0}{\bar{Y}(z,0)} = K_c\left[\frac{(z-z_{0Y})}{r_e}\right], \tag{9}$$

must be available. The constant K_c is the centreline decay rate and z_{0Y} is the intercept. Note that the intercept z_{0Y} is deliberately distinguished from the intercept, z_{0J}, obtained from the extrapolation of half-width data. Linear least-squares fitting of the centreline values of mass fraction was used to obtain the values summarized in table 4. The results are shown graphically in figure 4.

The rates of centreline decay for each of the gases are identical within experimental uncertainty. The mean value of K_c is 0.105 with a maximum observed difference of 2% between the highest and lowest values. This is in contrast to Niwa *et al.* (1984), Schefer & Dibble (1986) and Pitts (1991*a*), where a weak dependence of K_c on density ratio was reported. Possible sources for the discrepancy are discussed in the following section. Pitts (1991*a*) has provided an extensive compilation of values of K_c from previous investigations. The average value was $K_c = 0.105$ with an average deviation of ±10%. The mean value of K_c, 0.105, for the findings in table 4 compares quite well. Of interest to this investigation, Dowling & Dimotakis (1990) report K_c values of 0.98 for $Re = 5000$, and 0.106 for $Re = 16000$.

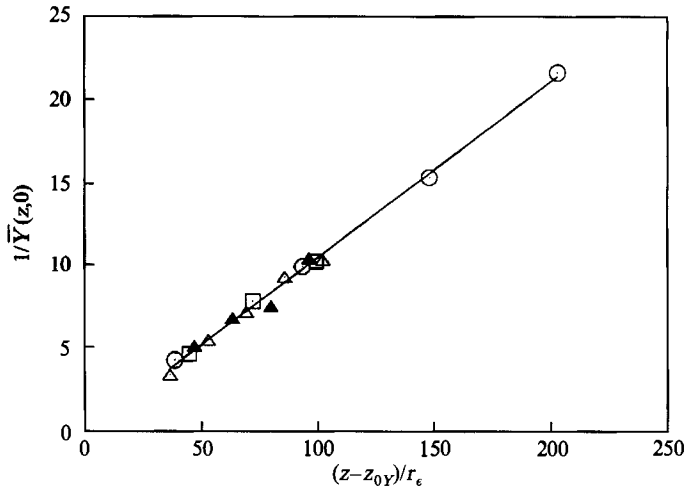

FIGURE 4. Plots of inverse centreline mass fraction versus downstream distance non-dimensionalized by r_ϵ are shown for the four jets. Symbols the same as figure 3.

From the observations of Pitts (1991*a*) and predictions of Thring & Newby (1953), values of z_{0Y} are expected to show a correlation with density. In a numerical study, So & Lui (1986) find similar trends for z_{0Y}. In the current study the methane value is greater than the propane value as expected. A similar trend for methane and propane jets was observed by Schefer & Dibble (1986). Because of its low density, the helium jet should have a virtual origin which is downstream of the other gases. The helium value derived from the current study is found to be out of sequence (see table 4). This is attributed to the additional dependence of z_{0Y} on *Re*. Pitts (1991*b*) has shown that there is a strong downstream shift of z_{0Y} with increasing *Re* over the range $Re = 4000$–25000. The helium jet *Re* is much lower than that for the propane and methane jets (4000 versus 25000), and consequently, z_{0Y} is expected to be shifted upstream as observed.

The rates of spreading and centreline decay can be used to test whether the jets investigated obey self-similarity by formulating the non-dimensional length scale η as the ratio $r/(z-z_0)$ and substituting in (4). If a Gaussian form is assumed for $f(\eta)$ (a good approximation except near the edge of the flow), then the mean mass fraction is given by

$$\bar{Y}(z,\eta) = \frac{r_\epsilon}{K_c(z-z_0)}\exp(-C\eta^2), \tag{10}$$

where C is a constant to be determined from experimental data. A straightforward transformation can be made from the jet spreading data using

$$(\ln 2/C)^{\frac{1}{2}} = \tan(\theta_c), \tag{11}$$

where θ_c the jet spreading half-angle discussed earlier.

The question of which value of z_0, i.e. z_{0J} or z_{0Y}, should be used in η and (10) arises. Comparison of table 4 to table 2 shows that the z_{0J} and z_{0Y} values are different for a given condition. The case of helium is presented since it has the largest difference between locations for the two virtual origins. The data were fit to the law given by (10) using the non-dimensional lengthscale $\eta = r/(z-z_{0Y})$, values of K_c and z_{0Y} obtained from the centreline decay law, and C calculated from (11). Fits to the helium data for $z/r_0 = 20$ and 80 are shown in figure 5. This approach gives a very poor collapse of the

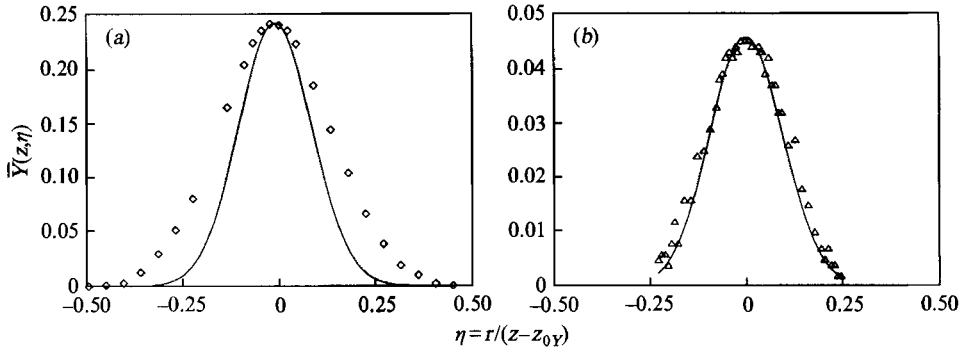

FIGURE 5. The similarity collapse of helium data, $\bar{Y}(z,\eta) = [K_c^{-1} r_\epsilon/(z-z_{0Y})]\exp(-C\eta^2)$, with $\eta = r/(z-z_{0Y})$; for (*a*) $z/r_0 = 20$ ($\diamond$) and (*b*) $z/r_0 = 80$ ($\triangle$).

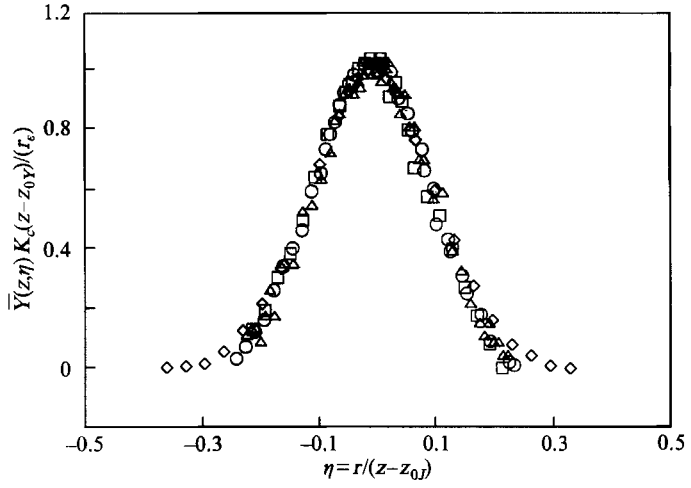

FIGURE 6. The similarity collapse of helium data, $\bar{Y}(z,\eta) = [K_c^{-1} r_\epsilon/(z-z_{0Y})]f(\eta)$, with $\eta = r/(z-z_{0J})$; $z/r_0 = 20$ ($\diamond$), 40 ($\bigcirc$), 60 ($\square$), and 80 ($\triangle$).

experimental data. The fact that the disagreement is so extreme at $z/r_0 = 20$ and less so at $z/r_0 = 80$ suggests that it is the scale $(z-z_{0Y})$ in the formulation of η that is responsible (i.e. the importance of z_0 diminsihes as z gets larger). Replacing z_{0Y} by the value of z_{0J} determined from the $r_{\frac{1}{2}}$ measurements in the expression for η while keeping the centreline scaling law (9), gives excellent collapse of the data shown in figure 6. Clearly, two different virtual origins are required in order for the helium data to obey similarity relationships. Interestingly, Grandmaison, Rathgeber & Becker (1982) observed a similar effect in their constant-density jet data and attributed it to 'non-idealities'. It is suggested that this effect was due to inaccurate specification of the virtual origin.

Results for the helium jet show that the mean mass fraction field is characterized properly by

$$\bar{Y}(z,\eta) = \frac{r_\epsilon}{K_c(z-z_{0Y})} f(\eta), \tag{12}$$

where $\eta = r/(z-z_{0J})$. The collapse of the results for the four jets investigated in this study by (12) is shown in figure 7(*a*) where all of the measurements are included. The

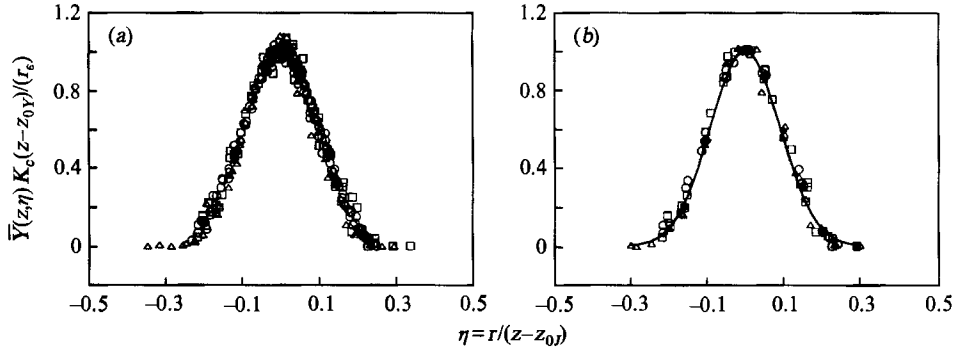

FIGURE 7. (*a*) The general similarity collapse of all data. (*b*) Selected results from (*a*) are shown along with data taken from Dowling & Dimotakis (1990) (◆) and values of $\bar{Y}(z,\eta)$ from (13) (solid curve).

agreement is excellent. In figure 7(*b*) selected data from figure 7(*a*) are compared with the constant-density measurements of Dowling & Dimotakis (1990). There is a close overlap of the variable-density and isodensity results. The functional form, $f(\eta)$, can be approximated by a Gaussian function (as shown in figure 7*b*) so that the mean scalar field of all axisymmetric free turbulent jets may be expressed as

$$\bar{Y}(z,\eta) = \frac{9.52 r_\epsilon}{z - z_{0Y}} \exp(-59\eta^2), \tag{13}$$

where the constant in the exponential term has been determined from a least-squares fit to all of the data. The expression given in (13) provides an excellent fit to all of the experimental data for $\eta < 0.15$. In the tail region the data drop off slightly faster than the Gaussian form for the locally collapsed data, as observed by others (Pitts & Kashiwagi 1984; Schefer & Dibble 1986).

A survey of the literature suggests that differing values of z_{0J} and z_{0Y} have been observed previously for axisymmetric jets. The significance of the observation, however, has not been addressed. A difference, between z_{0J} and z_{0Y}, is reported for a propane jet by Schefer & Dibble (1986). A similar effect can be identified in the results of So *et al.* (1990) by comparing their plots of the concentration centreline decay and concentration half-width.

In the literature the general descriptor 'virtual origin' is traditionally used for values which correspond to both z_{0J} and z_{0Y} as they are defined in this paper. In the classic similarity treatments of Hinze (1975) and Chen & Rodi (1980) it is assumed explicitly that the two virtual origins, z_{0J} and z_{0Y} are equal. The findings of this investigation demonstrate (as suggested by the literature cited above), however, that z_{0J} and z_{0Y} are not equivalent (at least in variable-density flows). Whether two different origins exist in constant-density flows is difficult to assess. Reports of the two values (in the same study) are scarce. Becker *et al.* (1967), for example, report both values to be the same in their constant-density flow as do Dowling & Dimotakis (1990). Grandmaison *et al.* (1982) in a study of very high *Re* (270000) constant-density jets report the two values to be identical as well. Plots of their data, however, show that z_{0J} and z_{0Y} are not equal.

The need for different virtual origins to describe self-similar behaviour has been observed in other types of flows. Two virtual origins are routinely employed to fit velocity data for plane turbulent jets to similarity relations (e.g. see Flora & Goldschmidt 1969; Hussain & Clark 1977; Chambers & Goldschmidt 1982; Browne *et al.* 1983; and Browne, Antonia & Chambers, 1984). In an experimental study of constant-density plane jets, Flora & Goldschmidt (1969) explicitly investigated the

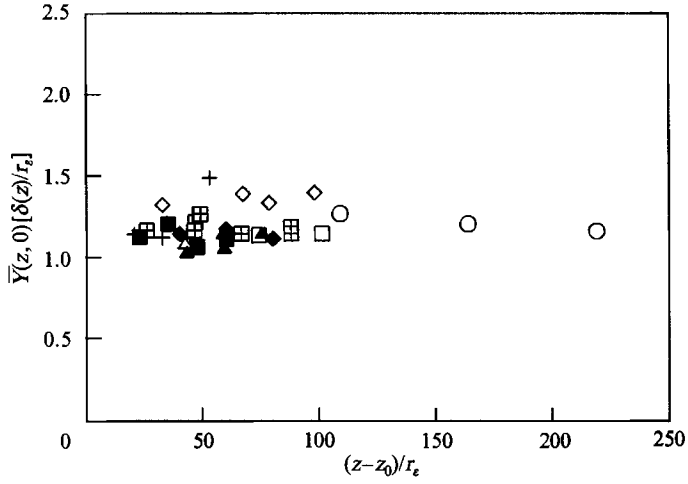

FIGURE 8. Centreline data for the four jets are plotted as $\bar{Y}(z,0)\,\delta(z)/r_\varepsilon$ versus $(z-z_0)/r_\varepsilon$. Symbols for current results are the same as figure 3. Literature findings: Schefer & Dibble (1986) (+), Papanicolaou & List (1988) (◇), Dowling & Dimotakis (1990) (⊞), So *et al.* (1990) (■), Becker *et al.* (1967) (◆).

existence of two virtual origins with regard to velocity. They identified two different virtual origins; one based on velocity half-width values, and the other on the decay of centreline velocity. The two axial positions were referred to as the 'geometric' and 'kinematic' origins, respectively. Absolute positions as well as the separation of the two virtual origins were shown to depend on the initial turbulence levels of the jets.

Browne *et al.* (1983, 1984) investigated both the velocity field and mixing of a passive scalar (temperature) in a plane jet. They found that both the velocity and scalar fields yielded different virtual origins when spreading rates or centreline falloff were considered, but that the virtual origins for each type of plot were coincident for the velocity and scalar. As generally observed, the spreading rate of the scalar was higher in the similarity region of the flow, with the ratio of the two widths being 1.23.

Two different virtual origins have also been observed by LaRue, Libby & Seshadri (1981) in an investigation of the thermal boundary layer downstream of a half-heated grid. They found that the virtual origins required to fit the spreading of the thermal boundary layer and the transverse profile of mean temperature flux to similarity forms were very different.

The analysis which leads to (4) treats the jet as a massless source of momentum. The justification for this is due to the entrainment behaviour of the flow field which ensures that total jet mass flux increases rapidly with downstream distance, and thus the initial mass flux becomes insignificant compared to the total jet mass flux as downstream distance is increased. There is, however, no physical reason why the mass and momentum fields in the near-field regions of the jets must develop in the same manner. Thus, the 'memory' of the jet with regard to the initial mass flux is incorporated into the values z_{0Y} required to apply the similarity laws.

It is possible to check the self-similar behaviour of the jets in a form which is independent of these virtual origins. If the flow is self-similar in concentration, then $\bar{Y}(z,0)\,\delta(z)/r_\varepsilon$ should be independent of z. The data are shown plotted in this manner in figure 8. The asymptotic behaviour of the data provides additional evidence that the jets included in this study do indeed obey self-similar relations. For comparison, results from other experimental studies are included. The results indicate that there is

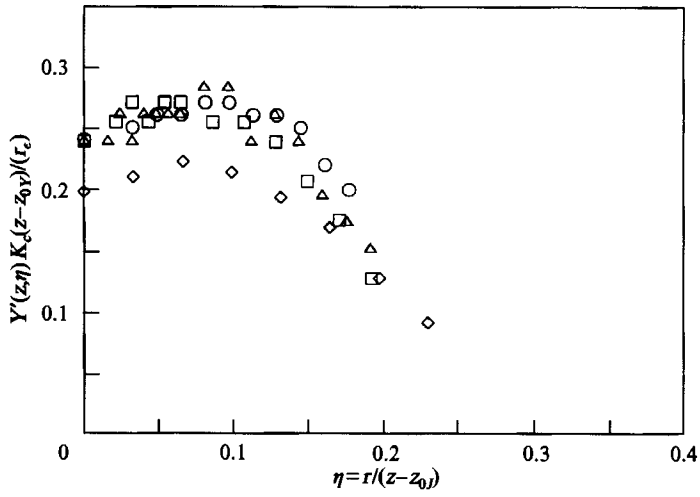

FIGURE 9. The general similarity collapse of helium concentration fluctuations, $Y'(z,\eta) = [K_c^{-1} r_e/(z-z_{0Y})]\,h(\eta)$, $\eta = r/(z-z_{0Y})$; $z/r_0 = 20$ (◇), 40 (○), 60 (□), and 80 (△).

disagreement as to what the asymptotic value for the constant is. Such variations are not surprising given the ranges in centreline decay and spreading rates which have been reported in the literature.

3.2. *Fluctuations of mass fraction*

The fluctuation behaviour of mass fraction has been characterized by calculating r.m.s. values from the real-time data. Results for helium are shown in figure 9. Note that the r.m.s. values are not normalized by centreline values. They are plotted in the same fashion as the mean data of figure 7,

$$Y'(z,\eta) = \frac{r_e}{K_c(z-z_{0Y})}\,h(\eta) \tag{14}$$

(that is, a form consistent with (12)). The collapse of the data is good for $z/r_0 > 20$. It is tempting to explain the low values at $z/r_0 = 20$ by concluding that r.m.s. values require a longer flow distance than mean values to approach self-preservation. Dowling & Dimotakis (1990) point out, however, that inadequate temporal and spatial resolution can lead to underestimation of r.m.s. values. A dimensionless frequency based on the spatial resolution of the probe voloume and the convection timescale of the jet was estimated from the experimental parameters. Comparison to the spectra reported by Dowling & Dimotakis (1990) indicates that at $z/r_0 = 20$ the r.m.s. values of mass fraction are indeed underestimated due to limited temporal and spatial resolution. Further support for this conclusion can be drawn from the observation that the tails of the r.m.s. profile at $z/r_0 = 20$, where the velocity has dropped off and thus resolution is better, fall into line with the other profiles.

The collapsed data for all of the gases and corresponding least-squares fits are shown in figure 10. All of the r.m.s. measurements are plotted in terms of the similarity parameters determined from the average concentration measurements, and are compared to isodensity measurements taken from Dowling & Dimotakis (1990). The solid line is a fourth-order polynomial fit to all of the data. The specification for the curve is

$$Y'(z,\eta) = \frac{9.52 r_e}{z-z_{0Y}}[0.23 + 0.35\eta + 9.09\eta^2 - 116.48\eta^3 + 240.81\eta^4], \tag{15}$$

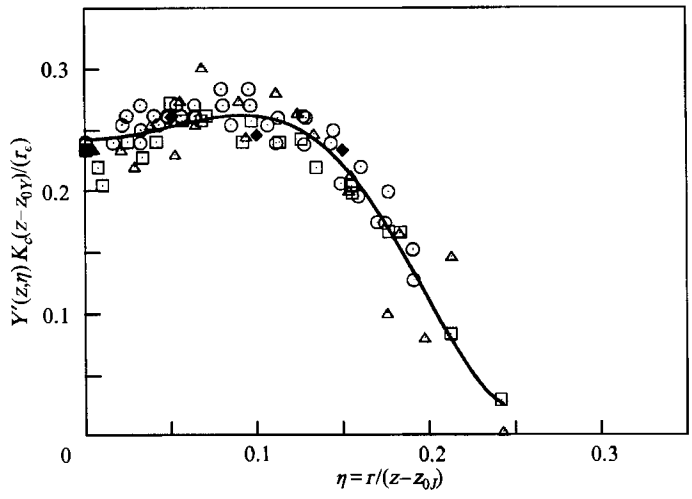

FIGURE 10. The similarity collapse of concentration fluctuations for all gases, $Y'(z,\eta) = [9.52r_\epsilon/(z-z_{0Y})]\,h(\eta)$, $\eta = r/(z-z_{0J})$; helium (○), methane (□), propane (△) and data taken from Dowling & Dimotakis (1990) (◆) and values of $Y'(z,\eta)$ from (15) (solid curve).

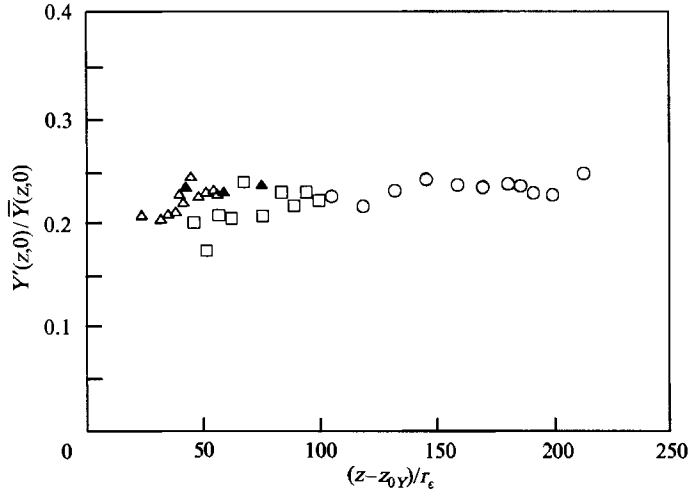

FIGURE 11. Behaviour of centreline unmixedness, $Y'(z,0)/\bar{Y}(z,0)$, for all gases: helium (○), methane (□), propane pipe (△), and propane nozzle (▲).

where $\eta = r/(z-z_{0J})$. All of these data show excellent agreement and are identical within experimental uncertainty, indicating that the concentration fluctuations in all of these jets obey the similarity relationship specified by (15).

The ratio of the r.m.s. to mean mass fraction, commonly referred to as the unmixedness (Hawthorne, Weddell & Hottel 1949), along the *centreline*, $Y'(z,0)/\bar{Y}(z,0)$, is plotted in figure 11. Since both $\bar{Y}(z,\eta)$ and $Y'(z,\eta)$ have been shown to collapse in a manner consistent with full self-preservation, their ratio is expected to be a constant. This is confirmed by the data of figure 11; the average value of unmixedness is 0.227 ± 0.011. This value compares well with those reported by Dowling & Dimotakis (1990) of 0.237 ± 0.005 for $Re = 16000$ and 0.230 ± 0.007 at $Re = 5000$. Based on their review of the literature Chen & Rodi (1980) recommend values of 0.21

to 0.24. Pitts (1991*a*) reports an asymptotic value of 0.23 for variable-density jets with a wide range of density ratio consistent with the current findings. Many other measurements of centreline unmixedness are available in the literature. These are summarized in Pitts (1991*a*). As was the case for time-averaged concentration, a wide range of values and behaviour have been reported and there is no apparent correlation with R_ρ or Re.

On the basis of the current findings, it is concluded that constant- and variable-density axisymmetric jets in the momentum-dominated regime attain a common asymptotic unmixedness.

4. Conclusions

The results of this study support the hypothesis that the final asymptotic state of *all* momentum-dominated axisymmetric jets depends only on the rate of momentum addition. Regardless of the initial conditions, axisymmetric turbulent free jets decay at the same rate (K_c), spread at the same half-angle (θ_c), and both the mean and r.m.s. mass fraction values collapse in a form consistent with *full* self-preservation.

There are many discrepancies in the literature concerning the centreline decay rate, spreading behaviour, attainment of an asymptotic centreline unmixedness value, and self-preservation behaviour in variable-density jets. This study has demonstrated that if a systematic experimental programme is undertaken in which care is taken to ensure that the flows are uncontaminated by buoyancy and coflow effects then the far-field behaviour of variable-density jets is essentially indistinguishable from a constant-density jet. This is supported by the excellent agreement for both the mean and r.m.s. values of this study with those of the constant-density experiment of Dowling & Dimotakis (1990).

The major conclusions concerning the concentration field of momentum-dominated axisymmetric jets with an initial density difference are:

(i) The centreline decay rate and spreading rate are independent of initial density ratio, velocity profile, and turbulence level.

(ii) The centreline unmixedness reaches an average asymptotic value of 0.227 regardless of initial density ratio.

(iii) Both means and fluctuations follow a law of *full* self-preservation in which two virtual origins must be specified. The collapse of data using this approach is in excellent agreement with others.

(iv) The virtual origin obtained from spreading data, z_{0J}, does not necessarily coincide with the virtual origin obtained from centreline decay rate, z_{0Y}.

The memory of the jet is embodied in the virtual displacements, z_{0J} and z_{0Y}. Once the displacements are specified, however, the flow fields collapse in a general manner. The dependence of z_{0J} and z_{0Y} on such system parameters as Re and R_ρ requires additional investigation. Also of interest is the coupling between the near-field development of the scalar and velocity fields and the behaviour of z_{0J} and z_{0Y}. Detailed velocity measurements should be performed in variable-density jets to fully characterize the self-preservation behaviour of this important class of flows.

The authors would like to acknowledge the three reviewers of this manuscript for their many thoughtful comments and suggestions for changes. Thanks to their efforts, a much improved paper appears here.

REFERENCES

ABRAMOVICH, G. N. 1963 *The Theory of Turbulent Jets.* MIT Press.

AVERY, J. F. & FAETH, G. M. 1975 Combustion of a submerged gaseous oxidizer jet in a liquid metal. *Fifteenth (Intl) Symp. Combust.*, pp. 501–512. The Combustion Institute.

BECKER, H. A., HOTTEL, H. C. & WILLIAMS, G. C. 1967 The nozzle-fluid concentration field of the round, turbulent, free jet. *J. Fluid Mech.* **30**, 285–303.

BIRCH, A. D., BROWN, D. R., DODSON, M. G. & THOMAS, J. R. 1978 The turbulent concentration field of a methane jet. *J. Fluid Mech.* **88**, 431–449.

BROWNE, L. W. B., ANTONIA, R. A. & CHAMBERS, A. J. 1984 The interaction region of a turbulent plane jet. *J. Fluid Mech.* **149**, 355–373.

BROWNE, L. W. B., ANTONIA, R. A., RAJAGOPANAN, S. & CHAMBERS, A. J. 1983 Interaction region of a two-dimensional turbulent plane jet in still air. In *Structure of Complex Turbulent Shear Flow* (ed. R. Dumas & L. Fulachier), pp. 411–419. Springer.

BRYNER, N., RICHARDS, C. D. & PITTS, W. M. 1992 A Rayleigh light scattering facility for the investigation of free jets and plumes. *Rev. Sci. Instrum.* **63**, 3629–3635.

CHAMBERS, F. W. & GOLDSCHMIDT, V. W. 1982 Acoustic interaction with a turbulent plane jet: effects on mean flow. *AIAA J.* **20**, 797–804.

CHEN, C. J. & RODI, W. 1980 *Vertical Turbulent Buoyant Jets – A Review of Experimental Data.* Pergamon.

DAHM, W. J. A. & DIBBLE, R. W. 1988 Coflowing turbulent jet diffusion flame blowout. *Twenty-Second (Intl) Symp. Combust.*, pp. 801–808. The Combustion Institute.

DAHM, W. A. & DIMOTAKIS, P. E. 1987 Measurements of entrainment and mixing in turbulent jets. *AIAA J.* **25**, 1216–1223.

DOWLING, D. R. 1991 The estimated scalar dissipation rate in gas-phase turbulent jets. *Phys. Fluids* A **3**, 2229–2246.

DOWLING, D. R. & DIMOTAKIS, P. E. 1988 On mixing and structure of the concentration field of turbulent jets. In *Proc. First National Congress on Fluid Dynamics, 25–28 July 1988 Cincinnati, Ohio. Part 2*, pp. 982–988. New York: AIAA.

DOWLING, D. R. & DIMOTAKIS, P. E. 1990 Similarity of the concentration field of gas-phase turbulent jets. *J. Fluid Mech.* **218**, 109–141.

FISCHER, H. B., LIST, E. J., KOH, R. C. Y., IMBERGER, J. & BROOKS, N. H. 1979 *Mixing in Inland and Coastal Waters.* Academic.

FLORA, J. J. & GOLDSCHMIDT, V. W. 1969 Virtual origins of a free plane turbulent jet. *AIAA J.* 7, 2344–2346.

GOULDIN, F. C., SCHEFER, R. W., JOHNSON, S. C. & KOLLMANN, W. 1986 Nonreacting turbulent mixing flows. *Prog. Energy Combust. Sci.* **12**, 257–303.

GRANDMAISON, E. W., RATHGEBER, D. E. & BECKER, H. A. 1982 Some characteristics of concentration fluctuations in free turbulent jets. *Can. J. Chem. Engng* **60**, 212–219.

HARSHA, P. T. 1971 Free turbulent mixing: a critical evaluation of theory and experiment. *Arnold Engineering Development Center Rep.* AEDC-TR-71-36.

HAWTHORNE, W. R., WEDDELL, D. S. & HOTTEL, H. C. 1949 Mixing and combustion in turbulent gas jets. *Third (Intl) Symp. Combust.*, pp. 266–288. The Combustion Institute.

HINZE, J. O. 1975 *Turbulence*, 2nd Edn. McGraw-Hill.

HINZE, J. O. & HEGGE ZIJNEN, B. G. VAN DER 1947 Transfer of heat and matter in the turbulent mixing zone of an axially symmetrical jet. *Appl. Sci. Res.* A **1**, 435–461.

HUSSAIN, A. K. M. F. & CLARK, A. R. 1977 Upstream influence on the near field of a plane turbulent jet. *Phys. Fluids* **20**, 1416–1426.

LARUE, J. C., LIBBY, P. A. & SESHADRI, V. R. 1981 Further results on the thermal mixing layer downstream of a turbulence grid. *Phys. Fluids* **24**, 1927–1933.

MORTON, B. R., TAYLOR, G. I. & TURNER, J. S. 1956 Turbulent gravitational convection from maintained and instantaneous sources. *Proc. R. Soc. Lond.* **234**, 1–23.

NAMAZIAN, M., SCHEFER, R. W. & KELLY, J. 1988 Scalar dissipation measurements in the developing region of a jet. *Combust. Flame* **74**, 147–160.

NIWA, C., ICHIZAWA, J., YOSHIKAWA, N. & OHTAKE, K. 1984 Time-resolved concentration measurements of jets by laser Rayleigh method-comparison of He, CO_2, and CCl_2F_2 jets. *Proc. Fourteenth Intl Symp. Space Tech. and Science, Tokyo*, pp. 469–476.

PAPANICOLAOU, P. N. & LIST, E. J. 1988 Investigations of round vertical turbulent buoyant jets. *J. Fluid Mech.* **195**, 341–391.

PITTS, W. M. 1991*a* Effects of global density ratio on the centerline mixing behavior of axisymmetric turbulent jets. *Expts Fluids* **11**, 125–134.

PITTS, W. M. 1991*b* Reynolds number effects on the centerline mixing behavior of axisymmetric turbulent jets. *Expts Fluids* **11**, 135–144.

PITTS, W. M. & KASHIWAGI T. 1984 The application of laser-induced Rayleigh light scattering to the study of turbulent mixing. *J. Fluid Mech.* **141**, 391–429.

SCHEFER, R. W. & DIBBLE, R. W. 1986 Mixture fraction measurements in a turbulent nonreacting propane jet. *AIAA Paper* 86-0278.

SCHLICHTING, H. 1979 *Boundary Layer Theory*, 7th Edn. McGraw-Hill.

SFORZA, P. M. & MONS, R. F. 1978 Mass, momentum, and energy transport in turbulent free jets. *Intl J. Heat Mass Transfer* **21**, 371–384.

SO, R. M. C. & LUI, T. M. 1986 On self-preserving, variable-density, turbulent free jets. *Z. Angew. Math. Phys.* **37**, 538–558.

SO, R. M. C., ZHU, J. Y. Z., OTUGEN, M. V. & HUANG, B. C. 1990 Some measurements in a binary gas jet. *Expts Fluids* **9**, 273–284.

SUNAVALA, P. D., HULSE, C. & THRING, M. W. 1957 Mixing and combustion in free and enclosed turbulent jet diffusion flames. *Combust. Flame* **1**, 179–193.

THRING, M. W. & NEWBY, M. P. 1953 Combustion length of enclosed turbulent jet flames. *Fourth (Intl) Symp. Combust.*, pp. 789–796. The Williams & Wilkins Co.

TOWNSEND, A. A. 1976 *The Structure of Turbulent Shear Flow*, 2nd edn. Cambridge University Press.

WHITE, F. M. 1974 *Viscous Fluid Flow*. McGraw-Hill.

WILSON, R. A. M. & DANCKWERTS, P. V. 1964 Studies in turbulent mixing – II a hot jet. *Chem. Engng Sci.* **19**, 885–895.